JETIR.ORG ISSN: 2349-5162 | ESTD Year : 2014 | Monthly Issue

JOURNAL OF EMERGING TECHNOLOGIES AND INNOVATIVE RESEARCH (JETIR)

An International Scholarly Open Access, Peer-reviewed, Refereed Journal

A review on the Variation in the properties of doped and undoped $MnFe_2O_4$ nanoparticles

Sudha Gulati

Department of Physics, Kalindi College, East Patel Nagar, New Delhi, India

Abstract : Manganese ferrite ($MnFe_2O_4$) nanoparticles are among the most significant magnetic metal oxide nanoparticles. The nanoparticles can be synthesised with a controllable crystallite size and shape using a variety of methods. In the present work, a review of research on the structural, electrical, and magnetic properties of doped and undoped $MnFe_2O_4$ nanoparticles, a promising candidate for diverse applications, is presented. The variation in structural, electrical, and magnetic properties is broadly attributed to the method of synthesis, deposition parameters, dopant, crystallite size and shape, orientation, grain boundaries, additional phases, lattice strain, cation distribution, exchange interactions between cations, and an inactive magnetic layer on the surface of nanoparticles, and this study of these properties is beneficial for optimising nanoparticles for diverse applications.

Keywords : $MnFe_2O_4$, nanoparticles, Structural properties, Crystallite size, Electrical Properties, Magnetic Properties

1. INTRODUCTION

Nowadays, society exhibits a growing inclination towards the utilisation of versatile smart materials with multiple functionalities. The area of materials research has garnered significant attention from scientists across all disciplines. Over the past few decades, nanotechnology and its practitioners have been actively involved in the development and fabrication of smart multifunctional materials, commonly referred to as nanomaterials. Nanoparticles (NPs) are ultrafine particles (sizes between 1 and 100nm). NPs have a high ratio of surface area to volume and are consequently more reactive, versatile, and durable than bulk materials. These characteristics confer limitless opportunities for enhancing the mechanical, electrical, and magnetic properties of NPs. NPs are primarily categorised as either organic or inorganic. The former including carbon nanotubes, liposomes, and fullerenes, and the latter including quantum dots and magnetic nanoparticles (MNPs). (Chen et al., 2016; Doll et al., 2013; Eslami-Farsani et al., 2014; Hedayatnasab et al., 2017; Khalili et al., 2016; Nath and Banerjee, 2013) Due to their ability to be functionalized on both the cellular and molecular levels, MNPs have acquired tremendous popularity.

Researchers have been drawn to magnetic materials, such as ferrites, due to their unique electrical and magnetic characteristics. Ferrites can be classified into various subclasses based on their magnetic strength, crystal structure, and kind. The main types of ferrites are: (i) spinel ferrites, (ii) hexagonal ferrites, and (iii) garnets (Borhan et al., 2023). Mn Nano-ferrites have been extensively investigated in light of their saturation magnetization, exceptional high electrical resistivity, and high permeability, low eddy current losses, favourable mechanical properties, enhanced biocompatibility which are necessary for the production of high-frequency transformers, high-density recording media, microwave devices, hyperthermia therapy, MRI contrast agents, and sensor applications (Doaga et al., 2013; Gulati et al., 2023; Popa et al., 2008; Shahid et al., 2017).

The general chemical formula for spinel ferrites is expressed as AB_2O_4, in which A positions are preferentially occupied by divalent cations and B sites are filled by trivalent cations (Jin and Miyazaki, 2012). Different parameters can influence the site preference for ion distribution at tetrahedral (A site) and octahedral (B site) sublattices in ferrites. Among these parameters are the atomic radii of the ions, the orbital preference for a certain coordination, and the temperature (Haralkar et al., 2012). The relative magnitude of ions in relation to the size of the lattice is the most influential factor. Trivalent ions are typically smaller than divalent ions because the formation of increased electrostatic attraction in the larger charge causes the outer orbits to contract(Haralkar et al., 2012). According to crystal field theory, tetrahedral sites (A sites) have a preference for d^0, $d^{5,}$ and d^{10} ions, whereas octahedral sites (B sites) prefer d^3 and d^8 ions (Silawongsawat et al., 2008).

$MnFe_2O_4$ nanoparticles can be synthesized using various methods, such as co-precipitation, sol-gel, hydrothermal synthesis, and thermal decomposition (Gulati et al., 2023; Popa et al., 2008; Shahid et al., 2017)(Jain and Gulati, 2023). The choice of synthesis method can influence the size, shape, and surface properties of the nanoparticles. When rare earth (RE) ions are substituted in manganese-based spinel ferrite systems, the unpaired electrons in the 4f subshell may cause changes to the system's properties through the occurrence of 4f-3d spin-orbit (L-S) coupling. As a result, RE elements are preferred by researchers over transition elements for substitution (Shahid et al., 2017; Song et al., 2010). When Dy^{3+} or other rare earth ions are substituted, the structure is predicted to be distorted, causing microstrain and changing the electrical characteristics. The net magnetization changes as a result of the 3d-4f (L-S) coupling's improved magnetic moment ordering (Stergiou and Litsardakis, 2014).

Numerous applications rely on the structural, magnetic, and electrical properties of magnetic nanoparticles, which are influenced by the type of nanoparticles and dopant used, synthesis methods, interaction between particles, hysteresis curves, particle size distribution, ac and dc conductivity and particle size and morphology of NPs. Thus, in the field of nanotechnology and nanoscience, researchers customise the properties of materials to make them appropriate for a specific application. The most recent investigations on the variation in the structural, electrical, and magnetic properties of $MnFe_2O_4$ were discussed in the present work.

2. PROPERTIES OF $MnFe_2O_4$ NANOPARTICLES

2.1 Structural Properties

$MnFe_2O_4$ nanoparticles have distinct structural properties due to their specific crystal structure. These properties influence their behavior and applications. $MnFe_2O_4$ nanoparticles adopt a spinel crystal structure, where divalent manganese (Mn^{2+}) ions occupy tetrahedral sites and trivalent iron (Fe^{3+}) ions occupy octahedral sites in a face-centered cubic arrangement (Goodarz Naseri et al., 2011). The surface properties of $MnFe_2O_4$ nanoparticles can be modified through functionalization, affecting their interactions with other materials and their behavior in various applications. During their creation, the phase purity and crystal growth of $MnFe_2O_4$ nanoparticles can be changed, which changes their properties and possible uses (Kafshgari et al., 2019). To comprehend the precise effect of dopants on the crystal structure of $MnFe_2O_4$ under their experimental conditions, structural characterization studies, such as X-ray diffraction and transmission electron microscopy, were performed.

The effect of dopants on the crystal structure of $MnFe_2O_4$, a spinel ferrite compound, can vary depending on the type and concentration of dopants. Dopants influence the lattice parameters of $MnFe_2O_4$, leading to changes in the unit cell size and shape. The substitution of Fe or Mn ions with other transition metal ions may cause lattice expansion or contraction. Arteaga-Cardona et al. investigated the effects of various metal ions (Co, Ni, Zn, and Fe) on the lattice parameters of $MnFe_2O_4$, showing changes in the unit cell dimensions (Arteaga-Cardona et al., 2019). The size, crystallographic characteristics, and magnetic properties of the ferrite nanoparticles were influenced by the injection of different metal ions. Dopants are reported to affect the distribution of cations (Mn and Fe ions) between the tetrahedral (A-site) and octahedral (B-site) positions in the spinel structure (Devi and Soibam, 2017; Raland et al., 2017). This can lead to non-ideal cation distribution and affect the properties of nanoparticles.

Table 1 lists the structural, electrical and magnetic properties manganese ferrite nanoparticles reported by various researchers. Structural properties of doped $MnFe_2O_4$ have been studied for transition metal ions Zn^{2+}, Fe^{2+}, Ni^{2+}, Co^{2+}, rare earth elements such as La^{3+}, Dy^{3+}, Ce^{3+}, Sm^{3+}, Gd^{3+}, Yb^{3+} etc. (Arteaga-Cardona et al., 2019; Baig et al., 2021, 2019; Gulati et al., 2023; Meena et al., 2021; Rashmi et al., 2017). The lattice constant is reported to decrease marginally as the Zn concentration rises; however, the disparity becomes significant only when the Zn concentration difference is substantial. This phenomenon can occur when a significant quantity of Zn^{2+} ions with small ionic radii (0.74 Å) substitute for Mn^{2+} ions with large ionic radii (0.93 Å) [Arulmurugan et al., 2005]. The crystallite size and lattice constant varied between 8.443Å and 8.409Å and 11.3nm and 8.5nm, respectively, when the amount of Zn varied from 0.099 to 0.409. The introduction of dopants induce lattice strain in $MnFe_2O_4$, leading to distortions in the crystal structure. This strain can be characterized using X-ray or neutron diffraction techniques. Fig 1 shows XRD pattern reported by Akhtar et al. They reported that the values of strain for undoped, Tb-doped, Gd-doped, Ce-doped, and Pr-doped Mn ferrite are 0.2305, 0.2079, 0.1897, 0.0844, and 0.1213, respectively. Depending on the type and concentration of dopants, additional phases may form alongside the $MnFe_2O_4$ spinel phase. These additional phases can significantly alter the crystal structure and properties (Rashmi et al., 2017). It is reported that a minute secondary phase, $DyFeO_3$, was formed, which corresponds to JCPDS# 00-019-0433 in Dy doped $MnFe_2O_4$ nanoparticles (Baig et al., 2019). This phase potentially obstructs crystal growth and is accountable for the reduction in crystallite size. Dopants introduce defects and vacancies in the crystal lattice of $MnFe_2O_4$. These defects can affect the crystal structure and alter the material's properties (Sivakumar et al., 2021). The variation in lattice parameter in rare earth doped $MnFe_2O_4$ influenced the change in density and cell volume. Baig et al reported the variation in crystallite size from 13.4nm to 11.5nm, density from 5.03 to 5.36 g/cm^3, and cell volume from 610.64 Å^3 to 613.65 Å^3 as the concentration of dopant Dy varied from x=0 to x=0.1 in $Dy_xMnFe_{2-x}O_4$ nanoparticles. The shifting in the peaks in x-ray diffraction has been observed by various researchers (shown in figure 1). The Rare earth elements are reported to exhibit a notable propensity to refill the octahedral site. This preference is primarily attributed to the larger size of these elements in comparison to the metal ions present at the octahedral site, Mn^{2+}, which occupy the octahedral sites [Ansari et al., 2018]. Thus the lattice constant of doped $MnFe_2O_4$ increases which results in distortion in the lattice and variations are also observed in crystallite size, density, strain, and cell colume [Baig et al, 2019, Alonzian et al, 2018]. However, reduction in lattice parameter was also observed in rare earth doped $MnFe_2O_4$ which might be due to incorporation of rare earth ions leads to iron defects as well as tetrahedral and octahedral symmetry distortion [Gulati et al., 2023]. Table 1 lists lattice parameter, crystallite size, density, strain and cell volume reported by various researchers clearly shows that dopant is influencing the structural properties of nanoparticles

2.2 Electrical Properties

Manganese ferrite nanoparticles exhibit diverse electrical properties that stem from their composition, crystal structure, and surface characteristics. These properties make them intriguing for various applications. The investigation of electrical properties has been conducted through the examination of the changes in direct current (dc) resistivity in relation to temperature, as well as the analysis of alternating current (ac) conductivity, dielectric constant, and dielectric loss with respect to temperature and frequency [Baig et al., 2021, Baig et al., 2019, Ansari et al., 2018, D'souza et al., 2016]. $MnFe_2O_4$ nanoparticles can exhibit electrical conductivity, with values influenced by factors like particle size, crystallinity, and doping.(Ansari et al., 2018) [13]. The dielectric properties of ferrites are reported to be influenced by various parameters, including the preparation method, chemical composition, grain structure or size, and the quantity and kind of dopants (Xiao et al., 2006). Ferrites are perfect for high-frequency applications due to their high resistivity values and minimal eddy current losses (Takadate et al., 1998). Mn ferrite can be used in a variety of products, including phase shifters, high-frequency transformer cores, resonators, computers, TVs, and mobile phones, sensors, energy storage devices because of their electrical properties which makes them significant from a commercial standpoint (Stanciulea et al., 1992; Sugimoto, 2004) (Manohar et al., 2021).

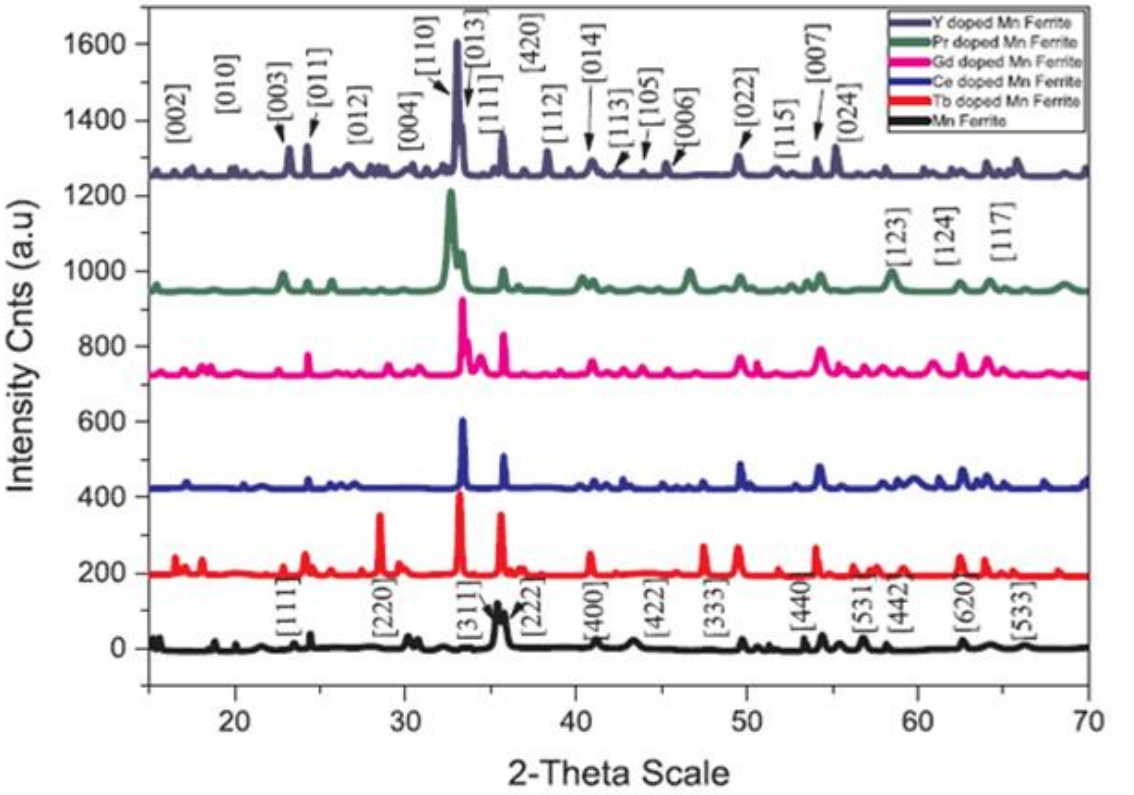

Figure 1 X-ray fiffraction patterns of $MnRE_{0.2}Fe_{1.8}O_4$ (RE = Tb, Pr, Ce, Y, Gd) nanoparticles. Reproduced from ref [Akhtar et al., 2018] with permission from Elsevier, copyright 2018.

$MnFe_2O_4$ nanoparticles have dielectric properties that vary with frequency and temperature, making them relevant for applications like microwave devices and capacitors (Singh Yadav et al., 2020). At nanoscale dimensions, $MnFe_2O_4$ particles might exhibit ferroelectric behavior, with polarization reversal under an applied electric field (Bhunia, 2022). $MnFe_2O_4$ nanoparticles can behave as semiconductors, with their electrical conductivity increasing with temperature. The electrical properties of $MnFe_2O_4$ nanoparticles can be tuned through methods like doping and controlled synthesis, enabling tailoring for specific applications (Jain et al., 2020). Doping $MnFe_2O_4$ nanoparticles can significantly alter their electrical properties, making them suitable for various applications.

Rare earth dopants, such as La, Ce, Nd, Pr, Nd, Eu, Gd, Cu, affect the electrical conductivity of $MnFe_2O_4$ (Ansari et al., 2018; Salah et al., 2012). Figure 2 shows that resistivity varies with temperature and dopant. The activation energy determined from figure 2 is reported to be in the range 0.28eV – 0.54eV. Alonzian et al reported the observed rise in DC resistivity (log ρ = 7ohm cm to 8.5 ohm cm) of $MnYb_xFe_{2-x}O_4$ nanoparticles upon the addition of Yb^{3+} ions (x increased from 0 to 0.1) which was attributed to the electron exchange phenomenon between Fe^{2+} ions and Fe^{3+} ions. An increase in temperature resulting in a decrease in the DC resistivity value provides confirmation that the nanoparticles that were prepared are semiconductors [Alonzian et al., 2018, Ansari et al., 2018]. The value of log ρ decreased from 8.7ohm cm to 5.7ohm cm with increase in temperature [Alonzian et al., 2018].

According to Salah et al, the structural properties of Cu-doped $MnFe_2O_4$ decrease with increasing electrical conductivity (Salah et al., 2012). These dopants introduce additional charge carriers and alter the electronic band structure, leading to variations in electrical conductivity. According to Batoo et al., whereas the loss tangent exhibits an aberrant behaviour with frequency for all compositions of Al-doped Mn ferrite, the dielectric constant exhibits a regular response with frequency (Mujasam Batoo, 2011). The dispersion phenomenon can be ascribed to the charge hopping process occurring between cations (Fe^{2+} and Fe^{3+}, Mn^{2+} and Mn^{3+}) situated at octahedral sites, as observed by the variation of dielectric characteristics and conductivity with frequency. Numerous articles have been published regarding the electrical characteristics of doped $MnFe_2O_4$, incorporating a range of divalent and trivalent metals. Fukuda et al. conducted a study on the electrical conductivity of Mn-Zn ferrite. According to their findings, the electrical conductivity of Mn-Zn ferrite exhibited a consistent and gradual rise in response to varying concentrations of Fe2+ ions (Fukuda et al., 2004). The electrical characteristics of Mn ferrite were investigated by Mazen et al. (Mazen et al., 1987). The researchers have observed that the electrical conductivity of manganese ferrite exhibits an upward trend as the level of cadmium replacement increases. The multiferroic behaviour of Ti-doped Mg-Mn ferrites was investigated by Shalendra et al. (Kumar et al., 2010). Their outcomes indicated that the substitution of Ti resulted in an increase in quadrupole interaction, while the hyperfine field exhibited a decrease. The substitution of Gd^{3+} in $MnFe_2O_4$ was reported to result in an increase in the ac conductivity, tan delta, and frequency-dependent dielectric constant. Samples exhibited dielectric constant as well as ac conductivity characteristics that were consistent with Maxwell–Wagner's model (Murugesan et al., 2015). The researchers observed that the dielectric loss exhibited an abnormal frequency dependency, while the dielectric constant displayed the expected behaviour in relation to frequency (Batoo et al., 2009). Reports have been presented regarding the investigation of the electrical properties of Ti-doped $MnFe_2O_4$ ferrite through the utilisation of ac impedance spectroscopy by varying the frequency within the range of 42 Hz to 5 MHz, and at different temperatures ranging from 300 to 473 K.

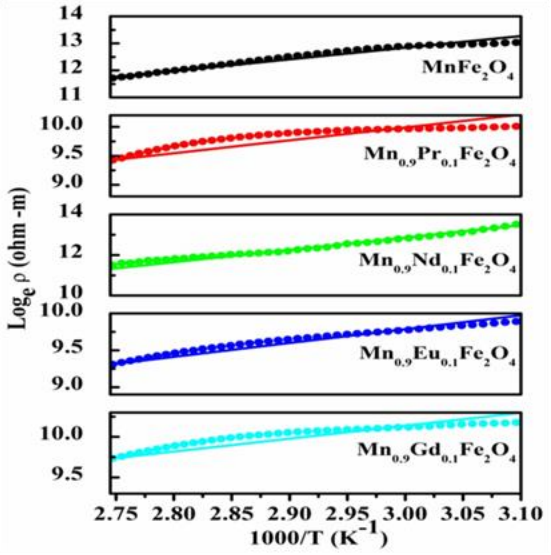

Figure 2 The variation of resistivity with temperature. Reproduced from ref [Ansari et al., 2018] with permission from Elsevier, copyright 2018.

The impedance spectra study reveals both the real and imaginary components of impedance exhibit a decreasing trend as the frequency increases. Additionally, it is observed that both the real and imaginary parts of impedance drop with Ti doping up to a concentration of 20%. However, above this threshold, there is a rise in both components, with additional increments in the Ti concentration. This experimental data has been modelled using two parallel RC equivalent circuits connected in series (Batoo et al., 2009). The dispersion phenomenon can be ascribed to the charge hopping process occurring between Fe $^{2+}$ and Fe^{3+} ions, as well as between Mn $^{2+}$ and Mn $^{3+}$ ions, which are situated at octahedral sites, as observed by the variation of dielectric characteristics and conductivity with frequency. A literature survey shows that dopants affect the concentration of charge carriers in $MnFe_2O_4$ nanoparticles, can influence the dielectric properties (dielectric constant and loss factor) of $MnFe_2O_4$ nanoparticles, can induce magnetoelectric coupling, shift $MnFe_2O_4$ nanoparticles from an insulating to a semiconducting regime, coupling between magnetic and electrical properties (Akhtar et al., 2018; Baig et al., 2021; D'souza et al., 2016). Table 1 depicts reported electrical properties of $MnFe_2O_4$. In order to elucidate the variation in dielectric parameters, the space charge polarisation mechanism was utilised. There was a decrease in these parameters as the frequency increased. The ferrite particles' low loss values at higher frequencies indicate their potential utility in the fabrication of high frequency microwave devices, among other applications [Baig et al., 2021]. The dielectric loss decreased from 0.85 to 0.32 at 3MHz for $MnFe_{2-x}La_xO_4$ nanoparticles at x=0.08. There are reports that dielectric losses are higher in the sample having larger lattice parameter for Dy doped $MnFe_2O_4$ nanoparticles [Baig et al., 2019].

2.3 Magnetic Properties

$MnFe_2O_4$ nanoparticles exhibit magnetic properties (Saturation magnetisation M_s, retentivity M_r, coercivity H_c, ,squareness ratio S = M_r/M_s, magnetic moment, anisotropy constant) due to their composition and crystal structure. The nanoparticles possess a spinel crystal structure where Mn^{2+} ions occupy tetrahedral sites and Fe^{3+} ions occupy octahedral sites. This arrangement leads to unequal magnetic moments between the two types of ions, resulting in a net magnetic moment (Hajalilou and Mazlan, 2016). $MnFe_2O_4$ nanoparticles exhibit relatively high saturation magnetization values, which makes them responsive to external magnetic fields (Ahalya et al., 2014; Judith Vijaya et al., 2015; Kumar et al., 2015). At nanoscale dimensions, $MnFe_2O_4$ nanoparticles can exhibit superparamagnetic behavior. $MnFe_2O_4$ nanoparticles can be engineered for biocompatibility and stability, enabling their use in biomedical applications without causing significant harm to biological systems (Asghar et al., 2020). The magnetic properties of $MnFe_2O_4$ nanoparticles make them suitable for magnetic hyperthermia, a cancer treatment where nanoparticles generate heat under alternating magnetic fields to selectively target and destroy cancer cells (Tartaj et al., 2003). The high magnetization of $MnFe_2O_4$ nanoparticles contributes to their use as contrast agents in magnetic resonance imaging, improving the visibility of tissues in imaging studies (Alonizan and Qindeel, 2018).

Table 1 : Structural, electrical and magnetic properties of doped and undoped $MnFe_2O_4$

Author	Material	Technique	Lattice parameter (Å)	Crystallite sizecs (nm)	Strain	Density (g/cm^3)	Cell Volume (Å^3)	M_s (emu/g)	M_r (emu/g)	M_r/M_s	H_c (Oe)	Mag Moment	Anis. Const. (erg/cm^3)	Real part of Dielectric constamt (ε′)	Imaginary part of Dielectric loss (ε″)	Tan loss	Variation of parameters/Frequency	Resistivity ρ(ohm-m)	Activation energy (E_a) (eV)
Arulmurugan, 2005	$Mn_{0.875}Zn_{0.099}Fe_{1.94}O_4$	Co-precipitation	8.442	11.3	-	-	-	42.4	1.99	-	12.8	-	-	-	-	-	-	-	-
	$Mn_{0.789}Zn_{0.21}Fe_{1.96}O_4$		8.44	10.8				48.1	1.45		9.02								
	$Mn_{0.699}Zn_{0.295}Fe_{1.98}O_4$		8.439	10.1				44.8	1.27		8.66								
	$Mn_{0.591}Zn_{0.399}Fe_{1.96}O_4$		8.436	9.2				35.1	0.717		8.58								
	$Mn_{0.499}Zn_{0.495}Fe_{1.99}O_4$		8.409	8.5				33.5	0.459		8.7								
Khaleghi, 2017	$Cu_xMn_{1-x}Fe_2O_4$ (x = 0, 0.3, 0.5)	Co-precipitation	-	35 - 42	-	-	-	42,36,30	-	-	-	-	-	-	-	-	-	-	-
Murugesan, 2015	$MnGd_xFe_{2-x}O_4$ (x=0.0, 0.05, and 0.1)	Sol-gel auto combustion	8.406, 8.4139, 8.4324	47	-	-	-	46.6, 44.6, 41	14, 9.9, 8.4	0.303, 0.222, 0.206	179.5, 153.5, 143	-	8713, 7131, 6101	12.75, 16.36, 19.86	-	0.25, 0.36, 0.39	130MHz		
Alonzian, 2018	$MnYb_xFe_{2-x}O_4$ (x = 0.00, 0.025, 0.05, 0.075, 0.10	Co-precipitation	8.28, 8.31, 8.34, 8.38, 8.61	53.34 48.63 41.83 6.652 8.77	-	4.31, 4.38, 4.43, 4.49, 4.61	-	25.65,21.45,19.31,16.25,13.4	-	0.43, 0.39, 0.38, 0.39, 0.36	-	-	28170, 48080, 62490, 67490, 7 0760	-	-	-	DC resistivity increases with x and decreases with increase of temperature	-	0.25 - 0.40
Author	**Material**	**Technique**	**Lattice parameter (Å)**	**Crystallite sizecs (nm)**	**Strain**	**Density (g/cm^3)**	**Cell Volume (Å^3)**	**M_s (emu/g)**	**M_r (emu/g)**	**M_r/M_s**	**H_c (Oe)**	**Mag Moment**	**Anis. Const. (erg/cm^3)**	**Real part of Dielectric const**	**Imaginary part of Dielectric**	**Tan loss**	**Variation of parameters/Frequency**	**Resistivity ρ(ohm-m)**	**Activation energy (E_a) (eV)**

														amt (ε′)	loss (ε″)				
Ansari, 2018	$MnFe_2O_4$	Sol-gel	8.4243	21.4		5.124		39.5	3.03	0.0767	36.11	1.63	-	-	-	-	-		2.03
	$Mn_{0.9}Pr_{0.1}Fe_2O_4$		8.4326	8.25		5.299		37.36	0.34	0.0091	4.53	1.6	-	-	-	-	-	-	0.19
	$Mn_{0.9}Nd_{0.1}Fe_2O_4$		8.4432	8.19		5.286		27.98	0.02	0.0007	0.48	1.2	-	-	-	-	-		0.52
	$Mn_{0.9}Eu_{0.1}Fe_2O_4$		8.4596	13.4		5.273		24.75	0.09	0.0036	1.75	1.06	-	-	-	-	-		0.16
	$Mn_{0.9}Gd_{0.1}Fe_2O_4$		8.4732	11.9		5.259		20.46	0.01	0.0004	0.59	0.88	-	-	-	-	-		0.14
Akhtar et al., 2020	Mn ferrite	Sol gel	a = 9.35069	61.1	0.2305		817.582	1.332	1.096	0.8228	425.23	0.183	590.01	-	-	-	-	-	-
	Tb doped Mn ferrite		a = 6.40075 c = 10.2458	80.5	0.2079		419.769	3.52	3.412	0.9693	310.4	0.876	1138.13						
	Gd doped Mn ferrite		a = 6.16336 c = 10.18545	64.3	0.1897		386.915	23.81	15.86	0.6661	339.6	4.327	8422.79						
	Ce doped Mn ferrite		a = 6.36124 c = 10.19182	68.5	0.0844		412.415	21.7	14.45	0.6658	246.1	5.8	5564.68						
Author	**Material**	**Technique**	**Lattice parameter (Å)**	**Crystallite size cs (nm)**	**Strain**	**Density (g/cm^3)**	**Cell Volume (Å^3)**	**M_s (emu/g)**	**M_r (emu/g)**	**M_r/M_s**	**H_c (Oe)**	**Mag Moment**	**Anis. Const. (erg/cm^3)**	**Real part of Dielectric constamt (ε′)**	**Imaginary part of Dielectric loss (ε″)**	**Tan loss**	**Variation of parameters/Frequency**	**Resistivity ρ(ohm-m)**	**Activation energy (E_a) (eV)**
	Pr doped Mn ferrite		a = 6.113	91.3	0.1231		384.328	7.021	5.459	0.7775	346.5	1.775	2534.14						

			38 c = 10.28348															
	Y doped Mn ferrite		a = 6.15995 c = 10.1808	95.2	0.1632		386.309	38.09	25.37	0.6662	330.2	10.54	13103.8					
Baig, et al.2019	$Dy_xMnFe_{2-x}O_4$ (x= 0.0, 0.01, 0.02, 0.04, 0.08, 0.16)	Surfactant assisted Chemical approach	8.4734	13.4		5.03	608.38	-	-	-	-	-	-	-	-	-	e', e" and Tandelta decreases with an increase in frequency for all samples/up to 3GHZ	-	-
			8.4839	11.6		5.04	610.64												
			8.4774	13.8		5.07	609.24												
			8.4811	16.17		5.11	610.04												
			8.4746	12.15		5.22	608.64												
			8.4978	11.5		5.36	613.65												
Sharma et al., 2021	$Mn_{0.5}Zn_{0.5}Cu_xFe_{2-x}O_4$ (x = 0.0,0.1, 0.2, and 0.3)	Solution combustion method	-	16 - 24	-	-	-	-	-	-	-	-	-	880–447		0.68 – 0.13	10^2 - 10^7 Hz	-	-
Author	**Material**	**Technique**	**Lattice parameter (Å)**	**Crystallite sizecs (nm)**	**Strain**	**Density (g/cm^3)**	**Cell Volume ($Å^3$)**	**M_s (emu/g)**	**M_r (emu/g)**	**M_r/M_s**	**H_c (Oe)**	**Mag Moment**	**Anis. Const. (erg/cm^3)**	**Real part of Dielectric constamt (ε′)**	**Imaginary part of Dielectric loss (ε″)**	**Tan loss**	**Variation of parameters/Frequency**	**Resistivity ρ(ohm-m)**	**Activation energy (E_a) (eV)**
Baig et al.,2021	$MnFe_{2-x}La_xO_4$, x=0	Reverse micelle	8.4304	12.82	-	-	-	-	-	-	-	-	-	4.71	0.73	0.13	1MHz	40.93×10^{-9}	-
	x=0.04		8.4438	14.21										11.82	0.73	0.04		86.35×10^{-12}	

	x=0.06		8.4861	15.58										7.24	0.44	0.07		21.80×10^{-10}	
	x=0.08		8.5067	15.95										10.74	0.73	0.06		20.76×10^{-10}	
	$MnFe_{2-x}La_xO_4$, x=0													4.53	0.44	0.08	2MHz		
	x=0.04													12.94	2.08	0.16			
	x=0.06													7.33	0.66	0.09			
	x=0.08													12	1.93	0.16			
	$MnFe_{2-x}La_xO_4$, x=0													4.42	0.51	0.85	3MHz		
	x=0.04													11.54	3.12	0.26			
	x=0.06													7.33	0.96	0.13			
	x=0.08													10.7	3.04	0.32			
Author	**Material**	**Technique**	**Lattice parameter (Å)**	**Crystallite sizecs (nm)**	**Strain**	**Density (g/cm^3)**	**Cell Volume (Å^3)**	**M_s (emu/g)**	**M_r (emu/g)**	**M_r/M_s**	**H_c (Oe)**	**Mag Moment**	**Anis. Const. (erg/cm^3)**	**Real part of Dielectric constamt (ε′)**	**Imaginary part of Dielectric loss (ε″)**	**Tan loss**	**Variation of parameters/Frequency**	**Resistivity ρ(ohm-m)**	**Activation energy (E_a) (eV)**
Sharma et al., 2022	$Mn_{1-x}Cu_xFe_2O_4$ (x = 0, 0.1, 0.2,0.3)	Solution combustion method	-	20.10 – 29.05	-	-	-	17.71 – 42.78	-	-	26.02–151.35	-	-	-	-	-	Dielectric constant shows anomalous behavior with Cu doping/10^2 -10^7 Hz	-	-
Jyoti et al., 2023	$Mn_{0.5}Zn_{0.5}VxFe_{2-x}O_4$ (x=0.0, 0.05, 0.10, 0.15, 0.20)	Solid state reaction method	8.4169, 8.4045, 8.4276, 8.4106,	11.15, 16.34, 15.59, 16.63, 13.93	0.039, 0.026, 0.026, 0.025, 0.029	5.701, 5.789, 5.701, 5.723, 5.777	596, 593, 598, 594, 593	44, 35, 30, 26, 24	12, 17, 12, 11, 13		137, 144, 130, 129, 131								

			8.4054															
Gulati et al.,2023	$MnFe_{2-x}Yb_xO_4$ nanoparticles (x = 0, 0.025, 0.075, 0.1, 0.15, and 0.2)	Co-precipitation	8.423 – 8.469	24.8 –34.7	-	0.039	-	64.4-26.5 at 300K, 88.1 - 58.3 at 5K	7.84-2.59 at 300K, 13.75 - 10.06 at 5K	0.12 - 0.09 at 300K, 0.16 - 0.18 at 3K	52 - 43 at 300K, 154 - 144 at 5K	2.66-1.21 at 300K, 3.64 - 2.65 at 3K	3417-1163 at 300K, 14133-8532 at 5	-	-	-	-	-	-

The magnetic characteristics of $MnFe_2O_4$ nanoparticles are influenced by the distribution of cations between tetrahedral and octahedral sites. $MnFe_2O_4$typically exhibits a normal spinel structure, with Mn^{2+} mainly occupying tetrahedral sites (Wang et al., 2016). The particle size of $MnFe_2O_4$nanoparticles influences their crystallinity and magnetic behavior. Smaller nanoparticles might exhibit superparamagnetic behavior due to thermal fluctuations (Patade et al., 2020). In comparison to the samples prepared at pH 3, 5, 7, and 9, the Mg–Mn ferrite sample prepared at pH < 1 exhibited a greater dielectric constant, reduced dielectric loss, and the highest values of Ms and Mr 30.04 emu/g and 4.93 emu/g, respectively (Lwin et al., 2015).

The inclusion of a transition metal ion with lower coercivity, such as nickel or iron, resulted in a decrease in the overall coercivity of the $MnFe_2O_4$(Arteaga-Cardona et al., 2019). Rare earth-doped manganese ferrite's magnetic properties can be attributed to a number of factors, including cation rearrangement, crystallite size, a lack of oxygen anions, exchange interactions between cations, and an inactive magnetic layer on the surface of nanoparticles (Akhtar et al., 2018; Ansari et al., 2018; Gulati et al., 2023). Doping with rare earth elements or other dopants can have a significant impact on the saturation magnetisation, coercivity, retentivity, magnetic moment, magnetic anisotropy, and hysteresis loss of $MnFe_2O_4$ nanoparticles, which are important parameters in magnetic materials.

Doping $MnFe_2O_4$ nanoparticles with rare earth elements like Dy, Nd, or Sm can enhance the coercivity of the material. Rare earth dopants introduce local magnetic moments that interact with the $MnFe_2O_4$ lattice, leading to an increase in coercivity (Shirsath et al., 2014). The type and concentration of rare earth dopants can be adjusted to fine-tune the coercivity of $MnFe_2O_4$ nanoparticles (Kolhatkar et al., 2013). Coercivity can also be influenced by the size and shape of $MnFe_2O_4$ nanoparticles. Rare earth dopants can interact differently with nanoparticles of varying sizes and shapes, leading to size-dependent effects on magnetic properties (Akhtar et al., 2018; Chandunika et al., 2020). Ansari et al reported coercivity values 36.11 Oe, 4.53 Oe, 4.48 Oe, 1.75 Oe and 0.59 Oe for undoped Mn ferrite, Pr, Nd, Eu, and Gd doped Mn ferrite respectively as shown in figure 3.

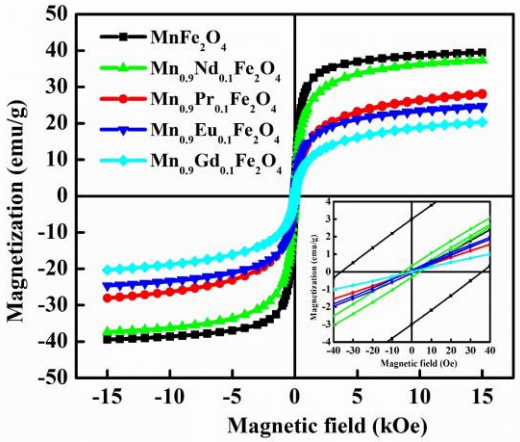

Figure 3 Hysteresis curves. Reproduced from ref [Ansari et al., 2018] with permission from Elsevier, copyright 2018.

Rare earth dopants can induce changes in the magnetic anisotropy of $MnFe_2O_4$ nanoparticles, which affect the direction of the magnetization and, consequently, the coercivity (Shahid et al., 2017). Dopants can modify the exchange interactions between magnetic ions in $MnFe_2O_4$ nanoparticles. These interactions influence the alignment of magnetic moments and can impact magnetic properties of MNPs (Gulati et al., 2023). Gulati et al observed higher values of K_a all the samples at a 5 K as compared to at 300 K which is due to increased saturation magnetization and coercivity values at reduced temperatures.

The magnetic properties, reported by various researchers, are listed in Table 1. Akhtar et al studied magnetic properties of $MnR_{0.2}Fe_{1.8}O_4$ (for Rare earth element R = Tb, Pr, Ce, Y and Gd) and concluded that Y-doped Mn ferrite is a more viable candidate for microwave regime applications involving switching and high frequency absorption. Ateia et al. investigated the rare earth ions (such as Dy^{3+}, Sm^{3+}, Gd^{3+}, La^{3+}, and Ce^{3+}) doped $MnZnFe_2O_4$ nanoparticles and discovered that these small substitutions influence the electrical and magnetic properties of doped ferrites and are classified as p-type semiconductors (Ateia et al., 2017). The effects of zinc substitution on the structural and magnetic characteristics of chemically derived nanosized manganese zinc mixed ferrites produced using the co-precipitation process were investigated by Gopalan et al.(Veena Gopalan et al., 2009). With zinc substitution (amount of Zn increased from 0 to 1), the magnetization of manganese ferrites was reported to gradually decrease from 57 to5.2, H_c decreased from 47 Oe to 0, and magnetic moment from 3.67 to 4.01. Murugesan et al. investigated the properties of Gd-doped manganese ferrite nanoparticles produced by a sol-gel technique and concluded that both saturation magnetization and coercivity decrease with an increase in Gd^{3+} substitution (Murugesan et al., 2015). The decrease in magnetisation with Gd^{3+} doping in $MnFe_2O_4$ was explained on the basis of magnetic moment determined from Neel model. The observed decreasing trend in H_c with increase in Gd^{3+} was ascribed to the confluence of the size effect and the magnetocrystalline anisotropy. The inclusion of rare-earth ions in a material is likely to result in magnetocrystalline anisotropy because of their relatively greater size in comparison to transition elements and their lower magnetic moment. Ahmed et al. investigated the effect of rare-earth ions on the magnetic properties of $Mn_{0.5}Zn_{0.5}R_{0.05}Fe_{1.95}O_4$ (R = 0, Tb, La, Ce and Th) and found that the addition of RE^{3+} ions enhanced the magnetic properties (Ahmed et al., 2007). Ahmed et al observed that the Curie temperature and effective magnetic moment were influenced by the rare earth element substitutions either through the partial diffusion of the rare earth element within the spinel lattice or through the formation of crystalline secondary phases, such as orthoferrite and/or garnet, along the grain boundaries. The reported values for the Curie temperature and magnetic moment were observed to fall within the range of 550 - 475 K and 5.45 - 3.38, respectively. The structural and magnetic properties of Ni-Mn-Cr ferrite nanoparticles (doped with Gd) revealed that coercivity and magnetization diminish as Gd content increases (Samoila et al., 2015). The impact of rare earth (Nd^{3+}) doping on the structural and magnetic characteristics of MnZn ferrite nanoparticles synthesised using the combustion process was investigated by Naik et al. (Naik et al., 2017). Their findings indicated that the introduction of Nd^{3+} doping resulted in an augmentation of saturation magnetization. The magnetic characteristics of $MnFe_2O_4$ nanoparticles are influenced by the distribution of cations between tetrahedral and octahedral

sites. There has been reports to explain variation in Ms on the basis of inactive or magnetic dead layer formed at the surface of nanoparticles (Gulati et al., 2023). The ratio t/cs (t is thickness of dead layer, cs is crystallite size) was calculated to increase from 0.03 to 0.11 with decrease in magnetisation from 64.4 to 26.5 when amount of Yb increased from 0 to 0.2 in $MnFe_2O_4$. Table 1 lists various values of squareness ratio S reported by researchers which indicated cubic anisotropy (S~0.83), uniaxial anisotropy (S~0.5), and uniaxial anisotropy with incomplete coupling (S <0.5). Literature survey shows that magnetic moment increased or decreased for different dopants in doped $MnFe_2O_4$ which indicated enhancement or reduction of super-exchange interactions.

3. CONCLUSIONS

The utilisation of manganese ferrite nanoparticles represents a noteworthy advancement in the field of magnetic metal oxide nanoparticles. The synthesis of this nanoparticle can be achieved using diverse processes, allowing for precise control over both the size and structure of the This paper presents a review pertaining to the variations in structural, electrical, and magnetic properties of both doped and undoped $MnFe_2O_4$ nanostructures. $MnFe_2O_4$ has emerged as a highly promising material for a wide range of applications, such as hyperthermia cancer therapy, magnetic resonance imaging, and energy conversion and storage devices. The broad range of structural, electrical, and magnetic properties exhibited by nanoparticles can be attributed to various factors, including the synthesis method, deposition parameters, dopant material, size and shape of the crystallites, the presence of additional phases, lattice strain, distribution of cations, exchange interactions between cations, and the presence of an inactive magnetic layer on the nanoparticle surface. Numerous researchers have correlated structural properties with the magnetic and electrical properties of Mn ferrite. The investigation and understanding of these properties are of great importance as they enable the optimisation of nanoparticles for a wide range of applications.

REFERENCES

1. K Ahalya, N Suriyanarayanan, S Sangeetha, (2014), Effect of pH and annealing temperatures on structural, magnetic, electrical, dielectric and adsorption properties of manganese ferrite nano particles. *Materials Science in Semiconductor Processing*, **27**, pp. 672–681.
2. M A Ahmed, N Okasha, M M El-Sayed, (2007) Enhancement of the physical properties of rare-earth-substituted Mn–Zn ferrites prepared by flash method. *Ceramics International*, **33**, pp. 49–58.
3. M N Akhtar, A B Sulong, M N Akhtar, M A Khan, (2018) Systematic study of Ce $^{3+}$ on the structural and magnetic properties of Cu nanosized ferrites for potential applications. *Journal of Rare Earths*, **36**, pp. 156–164.
4. N H Alonizan, R Qindeel, (2018) Structural and magnetic properties of ytterbium substituted spinel ferrites. *Appl. Phys. A*, **124**, pp. 408.
5. V.J. Angadi, L. Choudhury, K. Sadhana, H.-L. Liu, R.Sandhya, S. Matteppanavar, B. Rudraswamy, V. Pattar, R.V. Anavekar, K. Praveena, (2017), Structural, electrical and magnetic properties of $Sc^{3?}$ doped Mn–Zn ferrite nanoparticles. J. Magn. Magn. Mater. **424**, pp. 1–11.
6. M M N Ansari, S Khan, N Ahmad, (2018) Effect of R^{3+} (R = Pr, Nd, Eu and Gd) substitution on the structural, electrical, magnetic and optical properties of Mn-ferrite nanoparticles. *Journal of Magnetism and Magnetic Materials*, **465**, pp. 81–87.
7. F Arteaga-Cardona, U Pal, J María Alonso, P de la Presa, M E Mendoza-Álvarez, U Salazar-Kuri, M A Méndez-Rojas, (2019) Tuning magnetic and structural properties of $MnFe_2O_4$ nanostructures by systematic introduction of transition metal ions M^{2+} (M = Zn, Fe, Ni, Co). *Journal of Magnetism and Magnetic Materials*, **490**, pp 165496.
8. R. Arulmurugan, B. Jeyadevan, G. Vaidyanathan, & S. Sendhilnathan. (2005). Effect of zinc substitution on Co–Zn and Mn–Zn ferrite nanoparticles prepared by co-precipitation. *Journal of Magnetism and Magnetic Materials*, *288*, pp 470-477.
9. K Asghar, M Qasim, D Das, (2020) Preparation and characterization of mesoporous magnetic $MnFe_2O_4$@mSiO2 nanocomposite for drug delivery application. *Materials Today: Proceedings*, **26**, pp. 87–93.
10. E E Ateia, A A El-Bassuony, G Abdelatif, F S Soliman, (2017) Novelty characterization and enhancement of magnetic properties of Co and Cu nanoferrites. *J Mater Sci: Mater Electron*, **28**, pp. 241–249.
11. M M Baig, M A Yousuf, M F Warsi, P O Agboola, M Sher, I Shakir, (2019) Surfactant assisted synthesis of rare earth Dy^{3+} substituted $MnFe_2O_4$ nanoparticles. *Ceramics International*, **45**, pp. 18014–18022.
12. M M Baig, M A Yousuf, S Zulfiqar, A Safeer, P O Agboola, I Shakir, M F Warsi, (2021) Structural and electrical properties of La $^{3+}$ ions substituted $MnFe_2O_4$ ferrite nanoparticles synthesized via cost-effective reverse micelles strategy. *Mater. Res. Express*, **8**, pp. 035002.
13. M.M. Baig, M.A. Yousuf, M.F. Warsi, P.O. Agboola, M. Sher, I. Shakir, (2019), Surfactant assisted synthesis of rare earth Dy^{3+} substituted $MnFe_2O_4$ nanoparticles, Ceramics International, doi: https://doi.org/10.1016/j.ceramint.2019.06.020.
14. K M Batoo, S Kumar, C G Lee, Alimuddin, (2009) Study of ac impedance spectroscopy of Al doped $MnFe_{2-2x}Al_{2-x}O_4$. *Journal of Alloys and Compounds*, **480**, pp. 596–602.
15. R Bhunia, (2022) Piezoelectric Materials-based Nanogenerators, in: Inamuddin (Ed.), Materials Research Foundations. *Materials Research Forum LLC*, pp. 61–116.
16. A I Borhan, D Ghercă, A R Iordan, M N Palamaru, (2023) Classification and types of ferrites, in: Ferrite Nanostructured Magnetic Materials. *Elsevier*, pp. 17–34. https://doi.org/10.1016/B978-0-12-823717-5.00026-7
17. R K Chandunika, R Vijayaraghavan, N K Sahu, (2020) Magnetic hyperthermia application of $MnFe_2O_4$ nanostructures processed through solvents with the varying boiling point. *Mater. Res. Express*, **7**, pp. 064002.
18. G Chen, I Roy, C Yang, P N Prasad, (2016) Nanochemistry and Nanomedicine for Nanoparticle-based Diagnostics and Therapy. *Chem. Rev.*, **116**, pp. 2826–2885.
19. E C Devi, I Soibam, (2017) Effect of Zn doping on the structural, electrical and magnetic properties of $MnFe_2O_4$ nanoparticles. *Indian. J. Phys.*, **91**, pp. 861–867.
20. A Doaga, A M Cojocariu, W Amin, F Heib, P Bender, R Hempelmann, O F Caltun, (2013) Synthesis and characterizations of manganese ferrites for hyperthermia applications. *Materials Chemistry and Physics*, **143**, pp. 305–310.
21. T A P F Doll, S Raman, R Dey, P Burkhard, (2013) Nanoscale assemblies and their biomedical applications. *J. R. Soc. Interface.*, **10**, pp. 20120740.

22. A D'souza, M Deepak Kumar, M Chatim, V Naik, P P Naik, R B Tangsali, (2016) Effect of Rare-Earth Doping on Magnetic and Electrical Transport Properties of Nanoparticle Mn–Zn Ferrite. *Adv. Sci. Lett.*, **22**, pp. 773–779. https://doi.org/10.1166/asl.2016.6966
23. R Eslami-Farsani, S M Reza Khalili, Z Hedayatnasab, N Soleimani, (2014) Influence of thermal conditions on the tensile properties of basalt fiber reinforced polypropylene–clay nanocomposites. *Materials & Design*, **53**, pp. 540–549.
24. Y Fukuda, S Nagata, K Echizenya, (2004) Electrical conductivity of MnZn ferrite single crystals with a small number of Fe^{2+} ions. *Journal of Magnetism and Magnetic Materials*, pp. 279, 325–330.
25. M Goodarz Naseri, E B Saion, H A Ahangar, M Hashim, A H Shaari, (2011) Synthesis and characterization of manganese ferrite nanoparticles by thermal treatment method. *Journal of Magnetism and Magnetic Materials*, **323**, pp. 1745–1749.
26. S Gulati, S Gokhale, V Luthra, (2023) Effects of Yb^{3+} Doping on Structural, Morphological, and Temperature Dependent Magnetic Properties of $MnFe_2O_4$ Nanoparticles. *J. Supercond. Nov. Magn.,* https://doi.org/10.1007/s10948-023-06534-3
27. A Hajalilou, S A Mazlan, (2016) A review on preparation techniques for synthesis of nanocrystalline soft magnetic ferrites and investigation on the effects of microstructure features on magnetic properties. *Appl. Phys. A*., pp. 122, 680.
28. S J Haralkar, R H Kadam, S S More, S E Shirsath, M L Mane, S Patil, D R Mane, (2012) Substitutional effect of Cr^{3+} ions on the properties of Mg–Zn ferrite nanoparticles. *Physica B: Condensed Matter*, **407**, pp. 4338–4346.
29. Z Hedayatnasab, F Abnisa, W M A W Daud, (2017) Review on magnetic nanoparticles for magnetic nanofluid hyperthermia application. *Materials & Design*, **123**, pp. 174–196.
30. A Jain, Y G Wang, N Wang, Y Li, F L Wang, (2020) Tuning the dielectric, ferroelectric and electromechanical properties of Ba0.83Ca0.10Sr0.07TiO3– $MnFe_2O_4$ multiferroic composites. *Ceramics International*, **46**, pp. 7576–7585.
31. R Jain, S Gulati, (2023) Influence of Fe^{2+} substitution on FTIR and Raman spectra of Mn ferrite nanoparticles. *Vibrational Spectroscopy*, **126**, pp. 103540.
32. H Jin, T Miyazaki, (2012) Soft Magnetism, in: The Physics of Ferromagnetism, Springer Series in Materials Science. *Springer Berlin Heidelberg, Berlin, Heidelberg*, pp. 305–338.
33. J Judith Vijaya, G Sekaran, M Bououdina, (2015)Effect of Cu^{2+} doping on structural, morphological, optical and magnetic properties of $MnFe_2O_4$ particles/sheets/flakes-like nanostructures. *Ceramics International*, **41**, pp. 15–26.
34. A. S. Jyoti,G. G. Biswas, M. R. Rana, S. Islam, M. E. Hossain, et al. (2023). Investigation of the Structural, Electrical and Magnetic Properties of Vanadium Substituted Mn-Zn Ferrites https://doi.org/10.21203/rs.3.rs-2893893/v1.
35 1. L A Kafshgari, M Ghorbani, A Azizi, (2019) Synthesis and characterization of manganese ferrite nanostructure by co-precipitation, sol-gel, and hydrothermal methods. *Particulate Science and Technology*, **37**, pp. 904–910.
36. M. Khaleghi, H. Moradmard, S.F. Shayesteh, (2017), Cation distributions and magnetic properties of Cu-doped nanosized $MnFe_2O_4$ synthesized by the coprecipitation method. IEEE Trans. Magn. **54**, pp. 1–5.
37. S M R Khalili, R E Farsani, N Soleimani, Z Hedayatnasab, (2016) Charpy impact behavior of clay/basalt fiber-reinforced polypropylene nanocomposites at various temperatures. *Journal of Thermoplastic Composite Materials*, **29**, pp. 1416–1428.
38. A Kolhatkar, A Jamison, D Litvinov, R Willson, T Lee, (2013) Tuning the Magnetic Properties of Nanoparticles. *IJMS*, **14**, pp. 15977–16009.
39. S Kumar, K M Batoo, R Prakash, H K Choi, B H Koo, J I Song, H Chung, H Jeong, C G Lee, (2010) Impedance spectroscopy study on Mn1+x Fe2−2x Ti x O4 (0⩽x⩽0.5) ferrites. *J. Cent. South Univ. Technol.*, **17**, pp. 1133–1138.
40. S Kumar, T J Shinde, P N Vasambekar, (2015) Study of conduction phenomena in indium substituted Mn–Zn nano-ferrites. *Journal of Magnetism and Magnetic Materials*, **379**, pp. 179–185.
41. N Lwin, R Othman, A F M Noor, S Sreekantan, T C Yong, R Singh, C -C Tin, (2015) Influence of pH on the physical and electromagnetic properties of Mg–Mn ferrite synthesized by a solution combustion method. *Materials Characterization*, **110**, pp. 109–115.
42. A Manohar, C Krishnamoorthi, C Pavithra, N Thota, (2021) Magnetic Hyperthermia and Photocatalytic Properties of $MnFe_2O_4$ Nanoparticles Synthesized by Solvothermal Reflux Method. *J. Supercond. Nov. Magn*., **34**, pp. 251–259.
43. S A Mazen, A E Abd-el-Rahlem, B A Sabrah, (1987) The structure and electrical conductivity of Mn-Cd ferrite. *J. Mater. Sci.*, **22**, pp. 4177–4180.
44. S Meena, K S Anantharaju, Y S Vidya, L Renuka, B Uma, S C Sharma, B D Prasad S S More, (2021) Enhanced sunlight driven photocatalytic activity and electrochemical sensing properties of Ce-doped $MnFe_2O_4$ nano magnetic ferrites. *Ceramics International*, **47**, pp. 14760–14774.
45. K Mujasam Batoo, (2011) Study of dielectric and impedance properties of Mn ferrites. *Physica B: Condensed Matter*, **406**, pp. 382–387.
46. C Murugesan, B Sathyamoorthy, G Chandrasekaran, (2015) Structural, dielectric and magnetic properties of Gd substituted manganese ferrite nanoparticles. *Phys. Scr.*, **90**, pp. 085809.
47. P P Naik, R B Tangsali, S S Meena, S M Yusuf, (2017) Influence of rare earth (Nd+3) doping on structural and magnetic properties of nanocrystalline manganese-zinc ferrite. *Materials Chemistry and Physics*, **191**, pp. 215–224.
48. D Nath, P Banerjee, (2013) Green nanotechnology – A new hope for medical biology. *Environmental Toxicology and Pharmacology*, **36**, pp. 997–1014.
49. S R Patade, D D Andhare, S B Somvanshi, S A Jadhav, M V Khedkar, K M Jadhav, (2020) Self-heating evaluation of superparamagnetic $MnFe_2O_4$ nanoparticles for magnetic fluid hyperthermia application towards cancer treatment. *Ceramics International*, **46**, pp. 25576–25583.
50. M Popa, P. Bruna, D Crespo, J M Calderon Moreno, (2008) Single-Phase $MnFe_2O_4$ Powders Obtained by the Polymerized Complex Method. *Journal of the American Ceramic Society*, https://doi.org/10.1111/j.1551-2916.2008.02501.x
51. R D Raland, D Saikia, C Borgohain, J P Borah, (2017) Heating efficiency and correlation between the structural and magnetic properties of oleic acid coated MnF_2O_4 nanoparticles for magnetic hyperthermia application. *J. Phys. D: Appl. Phys.*, **50**, pp. 325004.
52. S K Rashmi, H S B Naik, H Jayadevappa, C N Sudhamani, S B Patil, M M Naik, (2017) Influence of Sm^{3+} ions on structural, optical and solar light driven photocatalytic activity of spinel $MnFe_2O_4$ nanoparticles. *Journal of Solid State Chemistry*, **255**, pp. 178–192.

53. D Ravinder, K V Kumar, (2001) Dielectric behaviour of erbium substituted Mn-Zn ferrites. *Bull. Mater. Sci.*, **24**, pp. 505–509. https://doi.org/10.1007/BF02706722
54. L M Salah, A M Moustafa, I S A Farag, (2012) Structural characteristics and electrical properties of copper doped manganese ferrite. *Ceramics International*, **38**, pp. 5605–5611.
55. P Samoila, L Sacarescu, A I Borhan, D Timpu, M Grigoras, N Lupu, M Zaltariov, V Harabagiu, (2015) Magnetic properties of nanosized Gd doped Ni–Mn–Cr ferrites prepared using the sol–gel autocombustion technique. *Journal of Magnetism and Magnetic Materials*, **378**, pp. 92–97.
56. M Shahid, S Shafi, M F Aly Aboud, M F Warsi, M Asghar, I Shakir, (2017) Impacts of Co^{2+} and Gd^{3+} co-doping on structural, dielectric and magnetic properties of $MnFe_2O_4$ nanoparticles synthesized via micro-emulsion route. *Ceramics International*, **43**, pp. 14096–14100. https://doi.org/10.1016/j.ceramint.2017.07.146
57. A. Sharma, K.M. Batoo, O.M. Aldossary, S. Jindal, N.Aggarwal, G. Kumar, (2022), Investigation of dielectric, electrical and optical properties of copper substituted Mn–Zn nanoferrites. J. Mater. Sci. **32**, pp. 313–322.
58. S E Shirsath, M L Mane, Y Yasukawa, X Liu, A Morisako, (2014) Self-ignited high temperature synthesis and enhanced super-exchange interactions of Ho^{3+} –Mn^{2+} –Fe^{3+} –O^{2-} ferromagnetic nanoparticles. *Phys. Chem. Chem. Phys.*, **16**, pp. 2347–2357.
59. C Silawongsawat, S Chandarak, T Sareein, A Ngamjarurojana, S Maensiri, P Laoratanakul, S Ananta, R Yimnirun, (2008) Effect of Calcination Conditions on Phase Formation and Characterization of $BiFeO_3$ Powders Synthesized by a Solid-State Reaction. *AMR*, **55–57**, pp. 237–240.
60. R Singh Yadav, I Kuřitka, J Vilcakova, T Jamatia, M Machovsky, D Skoda, P Urbánek, M Masař, M Urbánek, L Kalina, J Havlica, (2020) Impact of sonochemical synthesis condition on the structural and physical properties of $MnFe_2O_4$ spinel ferrite nanoparticles. *Ultrasonics Sonochemistry*, **61**, pp. 104839.
61. A Sivakumar, S S J Dhas, P Sivaprakash, A I Almansour, R S Kumar, N Arumugam, K Perumal, S Arumugam, M B Dhas, (2021) Raman Spectroscopic and Electrochemical Measurements of Dynamic Shocked $MnFe_2O_4$ Nano-Crystalline Materials, https://doi.org/10.21203/rs.3.rs-759475/v1.
62. J Song, L Wang, N Xu, Q Zhang, (2010) Microwave electromagnetic and absorbing properties of Dy^{3+} doped MnZn ferrites. *Journal of Rare Earths*, **28**, pp. 451–455.
63. L Stanciulea, J Neamtu, M Feder, E Segal, P Cristea, L Gal, (1992) Considerations on the sintering of manganese-zinc ferrite for power applications. *J. Mater. Sci. Lett*., **11**, pp. 961–963.
64. C Stergiou, G Litsardakis, (2014) Structural and magnetic properties of yttrium and lanthanum-doped Ni-Co and Ni-Co-Zn spinel ferrites, *ELECTROCERAMICS XIV CONFERENCE, Bucharest, Romania*, pp. 117–122.
65. M Sugimoto, (2004) The Past, Present, and Future of Ferrites. *Journal of the American Ceramic Society*, **82**, pp. 269–280.
66. K Takadate, Y Yamamoto, A Makino, T Yamaguchi, I Sasada, (1998) Fine grained Mn–Zn ferrite for high frequency driving. *Journal of Applied Physics*, **83**, pp. 6861–6863.
67. P Tartaj, M a del P Morales, S Veintemillas-Verdaguer, T Gonz lez-Carre o, C J Serna, (2003) The preparation of magnetic nanoparticles for applications in biomedicine. *J. Phys. D: Appl. Phys.*, **36**, pp. R182–R197.
68. E Veena Gopalan, I A Al-Omari, K A Malini, P A Joy, D Sakthi Kumar, Y Yoshida, M R Anantharaman, (2009) Impact of zinc substitution on the structural and magnetic properties of chemically derived nanosized manganese zinc mixed ferrites. *Journal of Magnetism and Magnetic Materials*, **321**, pp. 1092–1099.
69. J.J. Vijaya, G. Sekaran, M. Bououdina, (2015), Effect of $Cu^{2?}$ doping on structural, morphological, optical and magnetic properties of $MnFe_2O_4$ particles/sheets/flakes-like nanostructures. Ceram. Int. **41**, pp. 15–26.
70. H Wang, Q Yao, C Wang, B Fan, Q Sun, C Jin, Y Xiong, Y Chen, (2016) A simple, one-step hydrothermal approach to durable and robust superparamagnetic, superhydrophobic and electromagnetic wave-absorbing wood. *Sci. Rep.*, **6**, pp. 35549.
71. H -M Xiao, X -M Liu, S -Y Fu, (2006) Synthesis, magnetic and microwave absorbing properties of core-shell structured hopping of charge between Fe^{2+} and Fe^{3e} as well as between Mn^{2+} and Mn^{3+} ions at octahedral sites/TiO_2 nanocomposites. *Composites Science and Technology*, **66**, pp. 2003–2008.